IN-SITU STRUCTURAL HEALTH MONITORING OF COMPOSITE-OVERWRAPPED PRESSURE VESSELS

Sandra M. Klute, Daniel R. Metrey, Naman Garg, Nur Aida Abdul Rahim
Luna Innovations Incorporated
3155 State Street
Blacksburg VA 24060

ABSTRACT

Currently, most composite pressure vessels must be recertified every 2-5 years via hydrostatic testing to confirm the structural integrity of the pressure vessel. The test requires pressurization in a fluid filled chamber with the global volumetric expansion compared to acceptance criteria. This requirement poses significant cost and time out-of-service issues across many industries. In this work, Luna has teamed with Worthington Industries (WI) - a leading commercial and military supplier of composite air flasks and contracted designer of 30 year flasks, with the objective of providing composite flasks with a built-in structural integrity assessment system that will eliminate the need for hydrotesting recertification. High-definition (HD) distributed strain sensing is used to monitor strain along the axis of circumferentially-wrapped embedded fiber optic sensors in composite-overwrapped pressure vessels (COPVs) during qualification testing and following blunt and highly localized damage events. Luna demonstrates that the use of strain sensors embedded in the composite flask during manufacture will allow rapid assessment of the composite flask structural integrity on-site, while the flask is still mounted in the rack. In addition to the potential for replacing hydrotesting, risk associated with the use of 30 year extended service life flasks will be mitigated by utilizing this efficient health monitoring capability to identify damage and weakened flask structure. The core technology behind Luna's HD strain measurement systems is Optical Frequency Domain Reflectometry (OFDR) technology, which allows continuous strain measurements at hundreds of gage locations per meter of fiber. Application of the sensor is directly integrated into current flask fabrication methods and the technology utilizes standard telecommunication optical fiber. Therefore, the added cost associated with the embedded sensor and interrogation equipment will be minimal when compared to the recertification costs currently required.

1. INTRODUCTION

1.1 Composite Overwrapped Pressure Vessels (COPVs)

Composite materials are the natural choice for lightweight construction of pressure vessels. These materials are highly versatile and can provide comparable or higher strength than traditional metals at a fraction of the weight; however, COPVs require unique design, manufacturing, and test specifications. Compared to all-metal vessels, composite pressure vessels require a much more complex mechanical understanding as a result of the non-isotropic nature of the material and the interplay between the composite overwrap and the inner metallic liner. Several significant differences exist between composite and metal vessels: 1) Composites of carbon, Kevlar®, and glass may be subject to a reduction in burst strength as a result of surface impact, 2) Composites are vulnerable to an effect known as stress rupture or static fatigue,

defined as a sudden and catastrophic failure of the overwrap while holding at a stress level below the ultimate strength for an extended period of time; this failure mechanism is complex, not well understood, and difficult to accurately predict prior to failure, and 3) Quantitative nondestructive testing methods used to screen for flaws in thick-walled vessels are not applicable to COPV designs [1].

1.2 COPV Failure Modes

In the event of a failure, COPVs may experience a catastrophic release of energy as a result of the high pressure of the stored gas, posing significant danger to equipment and personnel. The NASA Pressure Vessel & Fracture Control Board has identified four primary failure modes associated with COPVs: 1) Burst from over-pressurization, 2) Fatigue failure of the metallic liner, 3) Burst resulting from damage to the metallic liner or composite damage, and 4) Stress rupture of the composite overwrap [2]. Burst from over-pressurization can be mitigated by material certification and proof-testing during acceptance and recertification testing, although must also be operationally controlled. Fatigue failure of the metallic liner can sometimes be mitigated by inspection and testing. Damage to the metallic liner or composite may be detected through visual inspection, although subsurface damage may not be readily identifiable. Stress rupture data has been used to develop a stress reliability model which uses specific characteristics such as survived time at Maximum Operating Pressure (MOP), expected time at MOP, and the stress ratio, defined as the stress in the overwrap at the maximum expected operating pressure divided by the stress in the overwrap at burst [3]. Accurately determining the stress ratio is key to the stress reliability model.

1.3 COPV Methods of Inspection

Specific design and test criteria for COPVs, such as DOT-CFFC (Department of Transport – Carbon Filament Fiber Wrapped Cylinder) Basic Requirements (Fifth Edition), "Basic Requirements for Fully Wrapped Carbon-Fiber Reinforced Aluminum Lined Cylinders," (March 2007) and International Standard ISO 11119-2 (First Edition), "Gas Cylinders of Composite Construction-Specification and Test Methods-Part 2: Fully Wrapped Fibre Reinforced Composite Gas Cylinders with Load-Sharing Metal Liners," (May 15, 2002), exist and are being utilized. Design and test requirements make use of hydrostatic testing to screen for defects in the manufacturing process and damage to the vessel during its service life. The hydrotest currently requires volumetric expansion measurements must be made to within 1% of the total expansion, or 0.1 cubic centimeters (cc).

This work demonstrates the granularity that can be achieved with embedded distributed strain sensors in terms of providing detailed strain profiles over the entire operating pressure range of a COPV, enabling a built-in assessment of the structural integrity of the vessel even through damage events.

2. EXPERIMENTATION

2.1 COPV Fabrication

A typical COPV design, consisting of an aluminum liner that is considerably thin through the center of the cylindrical portion of the flask, was utilized for this study. This design accommodates Department of Transport (DOT) requirements that these flasks fail in this central

portion when evaluated in burst testing. Layers of high strength carbon fiber/epoxy composite are applied via filament winding over the liner, providing the vast majority of the structural strength. Finally, glass fiber/epoxy layers are added to improve impact damage resistance. This glass layer can also serve to isolate the somewhat conductive carbon fiber layer from seawater, preventing galvanic corrosion issues. The flask is then cured, followed by autofrettage, which is used to expand the aluminum liner against the composite overwrapping material.

An experimental 7,500 psi (51.7 MPa) service pressure version of a COTS flask (Model ALT 843X flask), manufactured by WI was utilized for this evaluation. This flask is roughly 0.7 m long, 15 cm in diameter, and has a 8275 cc water capacity. Fabrication of the flask used standard WI fabrication procedures. However, optical fiber was embedded within the flask during the manufacturing process and monitored for continuity. A compilation of photographs from flask fabrication at WI can be found as Figure 1. The filament winding process leads to the seamless integration of the optical fiber. The optical fiber application is automated as the fiber is applied in the same fashion as that of the structural reinforcing fiber. As indicated in Figure 2, optical fiber was applied in a hoop layer allowing for complete coverage over the critical cylindrical section; the flasks are designed to ensure burst failure in the cylindrical section as opposed to the ends per DOT specifications.

Figure 1. Compilation of photographs from flask manufacturing (clockwise from top left): Aluminum liner in filament winder, Application of carbon fiber/epoxy hoop layer, Application of optical fiber strain sensor (from reel above) simultaneously with carbon fiber/epoxy hoop layer, Application of helical carbon fiber/epoxy layer, Application of glass fiber/epoxy helical layer (for impact resistance), and Flask after completion of winding.

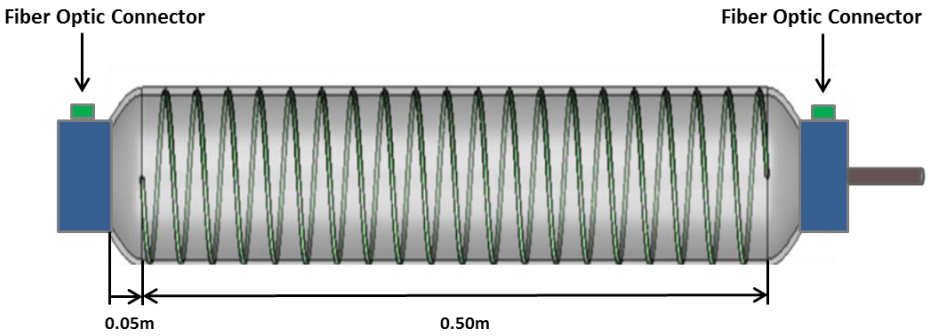

Figure 2. Schematic of embedded distributed strain sensor.

Most of the testing described below utilizes a distributed fiber optic strain sensor embedded within the COPV at the carbon fiber/glass fiber composite interface, on a diameter of approximately 15.4 cm covering a length of approximately 50 cm of the cylindrical portion of the flask. The total embedded sensor length was approximately 16 m. A second sensor was located approximately mid-way through the carbon composite. Placement of the strain sensors was performed simultaneously with application of the hoop wrap reinforcing fiber resulting in a 1.5 cm helix pitch, or spacing (referred to as bandwidth in filament winding) between each circumferential wrap of the sensor. The sensors are COTS telecommunications optical fiber. Both ends of the fibers were easily accessible for interrogation through connectors integrated into pressure vessel endcaps which were permanently bonded to the COPV.

2.2 Fiber Sensing Technique

The strain sensor is manufactured from standard off-the-shelf optical telecommunications fiber with a fused silica core and cladding and a protective coating, typically a polymer (although metals are possible). An individual sensor can be tens of meters in length and provide thousands of strain measurements at configurable points distributed along its length. Measurements are made using the Rayleigh scatter in the fiber, a random but stable pattern of reflections inherent to each fiber as a result of small-scale non-homogeneities. This random pattern of reflections is unique to each fiber and constant for the life of the fiber, forming a reflection signature unique to each sensor. Strain results in an apparent stretching of this signature, which translates to a shift in the spectral content of the pattern.

Sensors are interrogated using optical frequency domain reflectometry (OFDR), an interferometric technique which can distinguish sensors or scattering points at different locations along the fiber [4-6]. Figure 3 describes the basic OFDR network while Figure 4 walks through the steps taken to calculate strain. Light from a swept-tunable laser is split between the measurement path and a reference path by a fiber optic coupler. Light in the measurement path is sent to the sensor through the input path of an optical coupler. Light reflected from the sensor returns through the coupler and is recombined with light from the reference path. This combined signal then passes through a polarization beam splitter, which splits the light into orthogonal states recorded at the S and P detectors. A Fourier transform of these signals yields the phase and amplitude of the signal as a function of length along the sensor, i.e. the sensor signature.

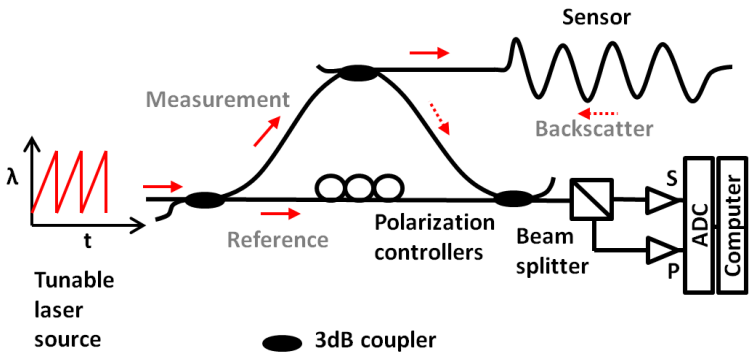

Figure 3. Basic OFDR optical network.

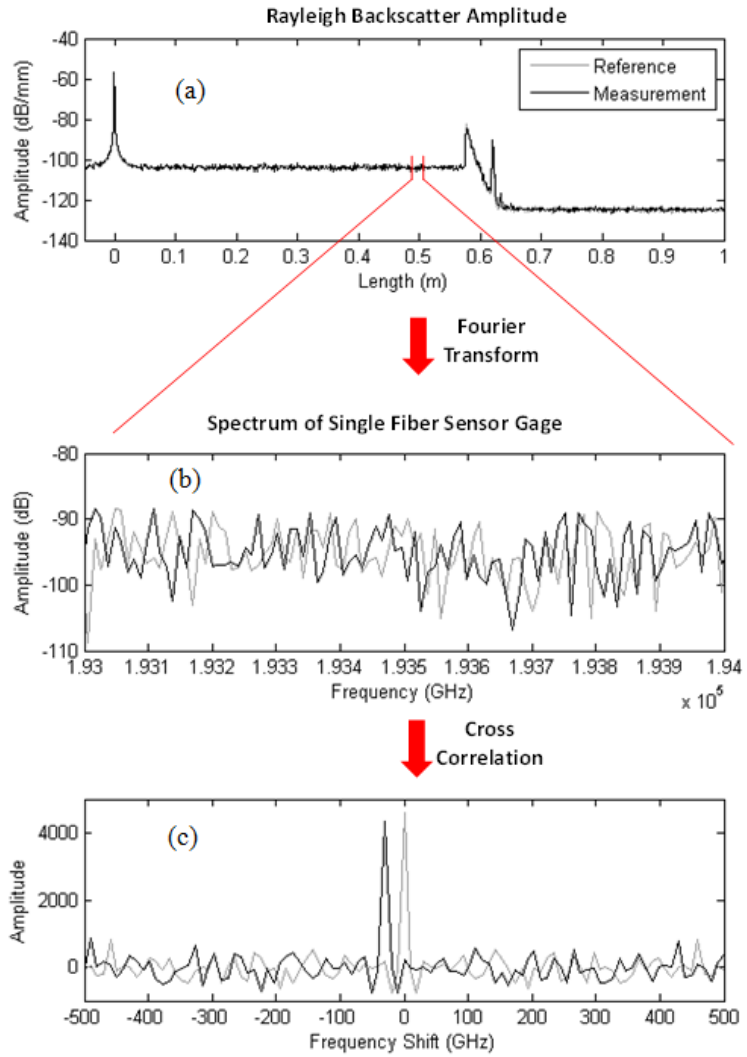

Figure 4. Frequency shift calculation from Rayleigh scatter measurement. (a) Rayleigh backscatter along optical path. (b) Spectrum of single sensor gage. (c) Cross-correlation of reference and measurement spectra.

To calculate strain, the spectral content of the sensor is compared between the measurement and reference state. Complex Fourier transform data is windowed around a desired measurement location (Figure 4 (a)). This window determines the gage length of the strain measurement. An inverse Fourier transform of the windowed data gives the spectral content from a particular gage in the sensor (Figure 4 (b)), which is cross-correlated (Figure 4(c)) with the spectrum from the same location of the sensor in a baseline state. Finally, the cross-correlated shift is converted to strain using an empirically determined calibration coefficient, or gage factor, analogous to that of the electrical strain gage. This process is repeated along the length of the sensor, forming a distributed measurement.

2.3 Test Sequence

The Model 843X flask, was tested at WI and standard hydrostatic test results compared with strain measurements from the embedded distributed strain sensors. A standard hydrotest was completed, recording the volumetric expansion at 12,500 psi (86.2 MPa) internal pressure. The flask was then removed from the hydrotest chamber and placed in WI's burst testing facility for pressurization of the flask past service pressure. Luna's commercially available Optical Backscatter Reflectometer (OBR), was used to interrogate the strain sensors embedded within the COPV and measurements recorded as the internal pressure of the flask was incrementally increased up to 12,500 psi and subsequently decreased back to 0 psi.

Following pressure testing an impact test was performed in which a small metal plate was held to the surface of the COPV and struck with a hammer to simulate blunt impact damage. The optical fiber sensor in the flask was interrogated and strain measurements recorded, after which another hydrotest was performed to determine whether structural damage to the COPV could be detected. This hydrotest was followed by a repeat of the strain-monitored pressure testing in the burst facility, incrementally measuring strain at pressures up to and down from 12,500 psi. This sequence (impact, hydrotest, and strain-monitored pressure testing) was repeated again after a more forceful tool impact.

After blunt impact testing, concentrated point damage was introduced to the COPV in the form of a 0.25 cm deep x 1 cm long slot milled into the composite overwrap at about the 0.35 m location as well as several sharp tool impacts at that same location. Distributed strain measurements were recorded as the COPV was pressurized up to 2,000 psi (13.8 MPa). A hydrotest was then performed to screen for damage detection.

3. RESULTS

3.1 Undamaged COPV

The COPV was subjected to pressurization in the Hydrostatic Test Facility at WI in which an autofrettage was performed, followed by a hydrotest at 12,500 psi (86.2 MPa) with a 60 sec hold, repeated 3 times. Results shown in Table 1 are within the expected range for this pressure vessel. The average total volumetric displacement at the 12,500 psi test point was 137.6 cc with a negligible average permanent deformation reading of 0.5 cc.

Table 1. Hydrostatic test results for pristine COPV 843X #X002 at 12,500 psi (86.2 MPa).

Serial # X002	Gage Pressure (psi)	TOTAL (cc)	PERM (cc)
Hydrotest 1	12,515	137.1	0.8
Hydrotest 2	12,525	137.6	0.6
Hydrotest 3	12,510	137.2	0.0
Hydrotest Avg.	12,517	137.3	0.5

Distributed strain measurements from the circumferentially embedded sensor are shown in Figure 5 at incremental pressure levels up to 12,500 psi. The strain responds linearly with pressure as expected, and tapers down to lower values as the ends of the cylindrical region are approached; in these regions the metal liner has been designed to be thicker, making the flask ends stiffer. The high spatial resolution of the strain sensor allows for examination of variation, or structure, in the strain data along the length of the cylinder, which appears consistent at each pressure level tested. In previous work it has been shown that structure in the composite strain measurements correlates with the composite weave (or over wrapping fiber) pattern [7-9]. The hydrotest data and distributed strain data for the undamaged COPV represent the baseline against which other measurements will be compared.

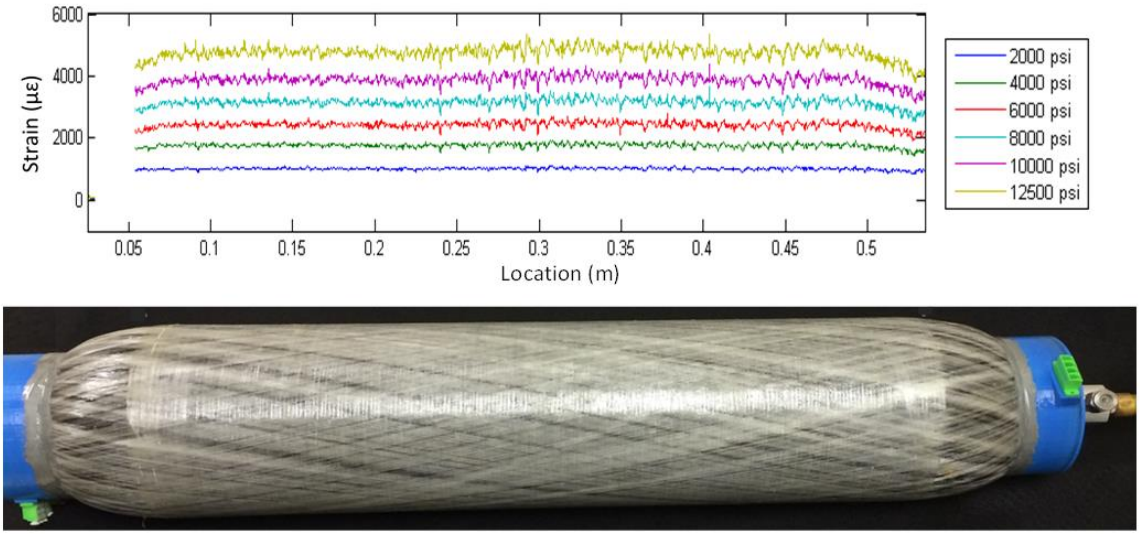

Figure 5. Distributed strain along sensor circumferentially embedded at carbon-glass interface of COPV over a range of pressures. 1000 psi = 6.9 MPa.

3.2 Blunt Impact Damage

The COPV was subjected to two blunt impact events at the same location, with the second being of higher severity than the first. Residual distributed strain along the length of the sensor is shown in Figure 6 as a function of COPV length for the unpressurized cylinder, where the effects of the impacts can clearly be seen. The periodic strain concentrations correspond to the sensor passing through the damaged region once per circumferential wrap, with each wrap spaced 1.5 cm apart. Impact 1 resulted in an affected area approximately 5 cm in length, while Impact 2 resulted in residual strain over a region of approximately 18 cm. A contour map of the strain

values after Impact 2 is shown in Figure 7. Strain concentrated regions of compression correspond to barely-visible indications of damage on the surface of the cylinder.

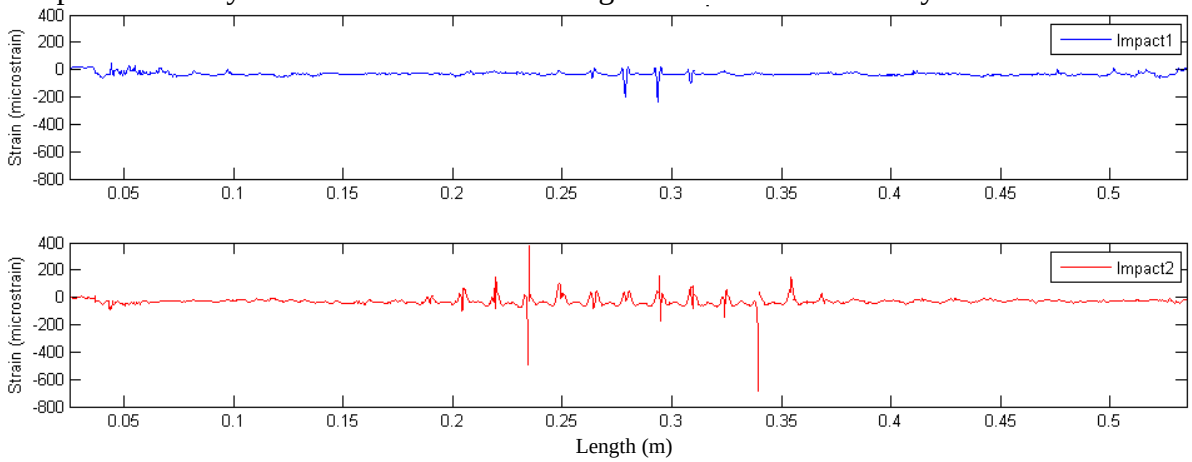

Figure 6. Residual strain along embedded sensor in unpressurized flask following two blunt impacts of increasing severity, as a function of length along the COPV.

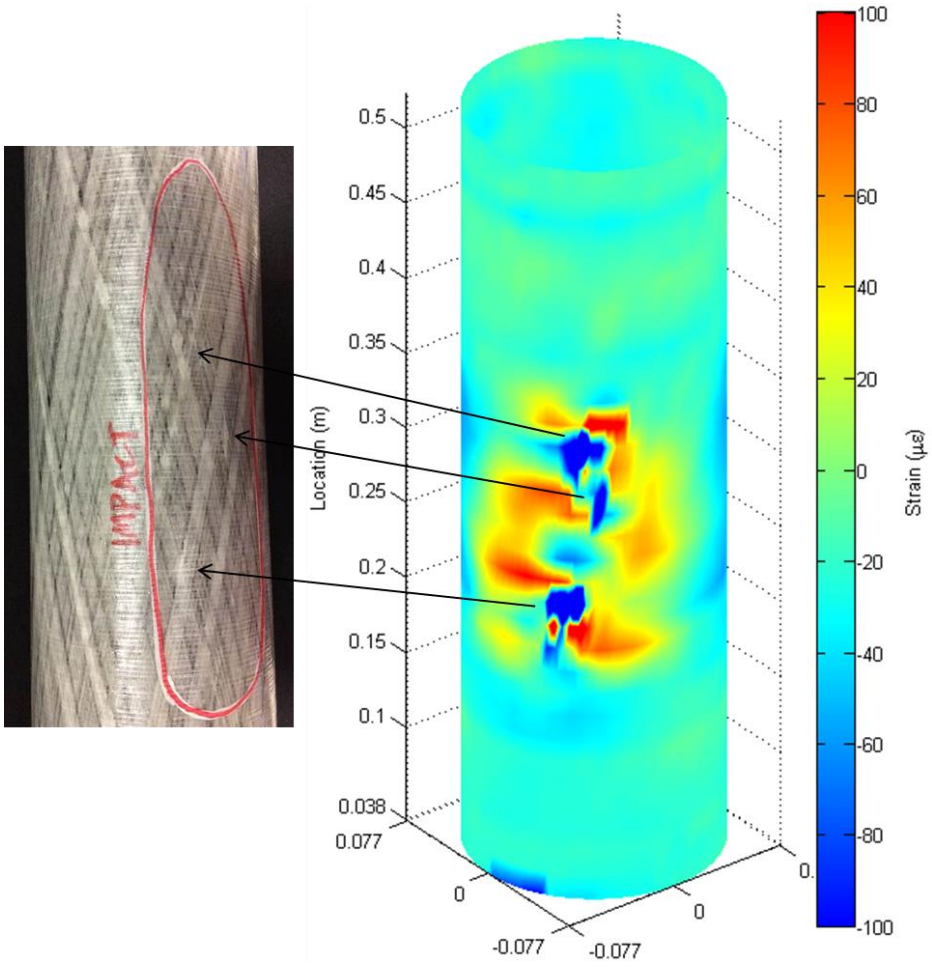

Figure 7. Contours of residual strain along circumferentially embedded sensor following blunt Impact 2.

Following each of the blunt impact damage events the CPOV was pressurized in the hydrotest facility to measure changes in volumetric displacement as well as the burst test facility to measure distributed strain. Results of the two post-impact hydrotests are presented in Table 2 and distributed strain measurements are shown in Figure 8 and Figure 10. Both post-impact hydrotests resulted in negligible changes in volumetric expansion compared with the test prior to impact (0.1 % and 0.8 %, respectively). The distributed strain profiles look similar as well, and the strain features appear repeatable over the three pressure cycles.

Table 2. Hydrotest results following two blunt impact damage events at 12,500 psi (86.2 MPa).

Impact 1 Hydrotest	Nominal Press. (psi)	TOTAL (cc)	PERM (cc)
Hydrotest 1	12,500	136.0	0.0
Hydrotest 2	12,500	139.1	1.8
Hydrotest 3	12,500	136.2	0.0
Impact 1 Hydro Avg.	12,500	137.1	0.6
Impact 2 Hydrotest	Nominal Press. (psi)	TOTAL (cc)	PERM (cc)
Hydrotest 1	12,500	136.8	0.5
Hydrotest 2	12,500	136.0	1.4
Hydrotest 3	12,500	135.8	-0.5
Impact 2 Hydro Avg	12,500	136.2	0.5

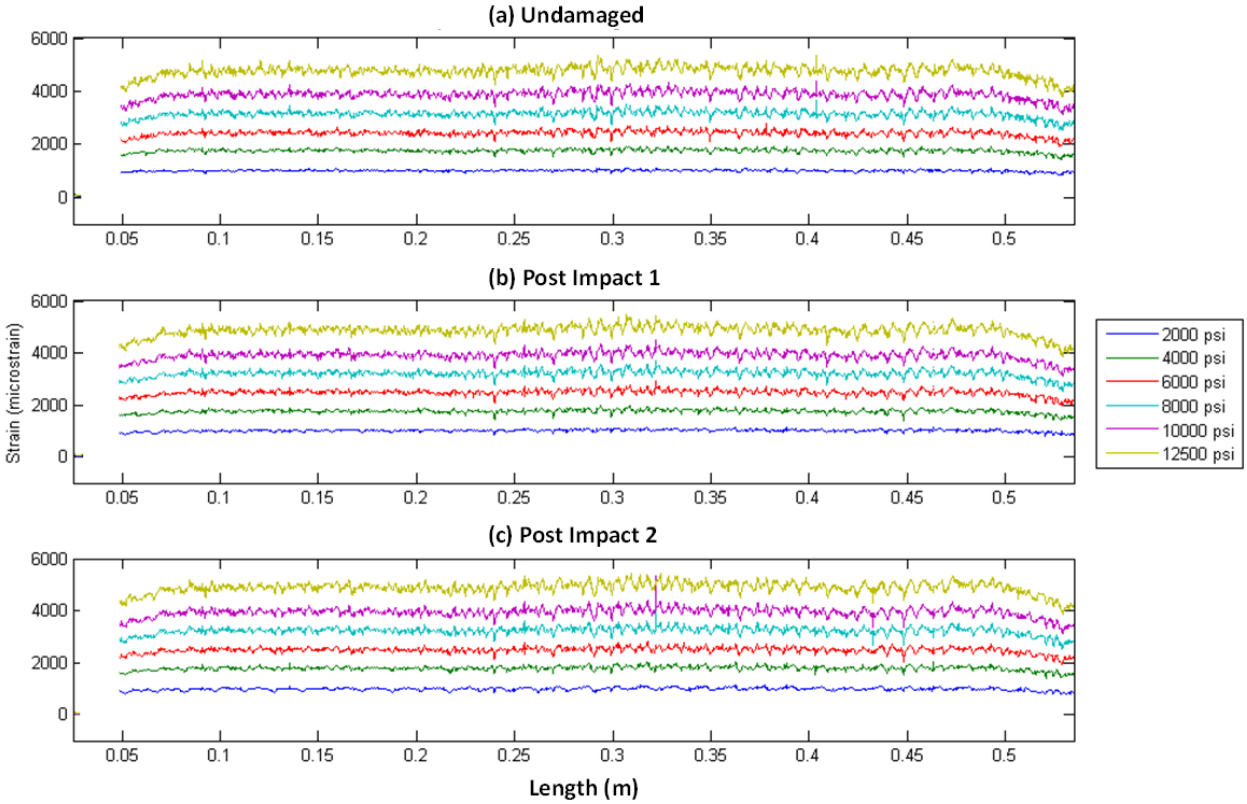

Figure 8. Distributed strain along circumferentially embedded sensor over a range of pressures (a) before damage, (b) after first blunt impact, and (c) after second blunt impact for comparison. 1000 psi = 6.9 MPa.

Figure 9 presents average strain measurements over the full pressure range for all three pressure cycles, taken over the center 2 m of the sensor. The strain varies linearly with pressure, and some apparent hysteresis appears in the comparison between the up and down cycles. A portion of this could likely be attributed to uncertainty in the actual gage pressure at each test point (estimated up to a couple hundred psi or 1.38 MPa uncertainty) or thermal effects on the strain measurement. Filling and pressurizing the flask introduced some heat into the pressure vessel, the amount of which slightly varied for each pressure cycle. Similar measurements in-service could be conducted within the same temperature range to negate the need for thermal compensation.

In Figure 10 we present strain profiles along the circumferentially embedded sensor as a function of pressure vessel length for 7,000 psi, the pressure test point closest to the vessel service pressure of 7,500 psi. Strain measurements from the undamaged vessel are compared with strain values after the two blunt impacts. The average strain values are plotted on the right, with bars representing the standard deviation of the structural strain resulting from the composite weave. The average strain values show weak growth by approximately 2 % and 2.8 % respectively in the post-impact tests. A close look at the structure to the strain pattern (inset of Figure 10) shows good agreement over all three pressure cycles.

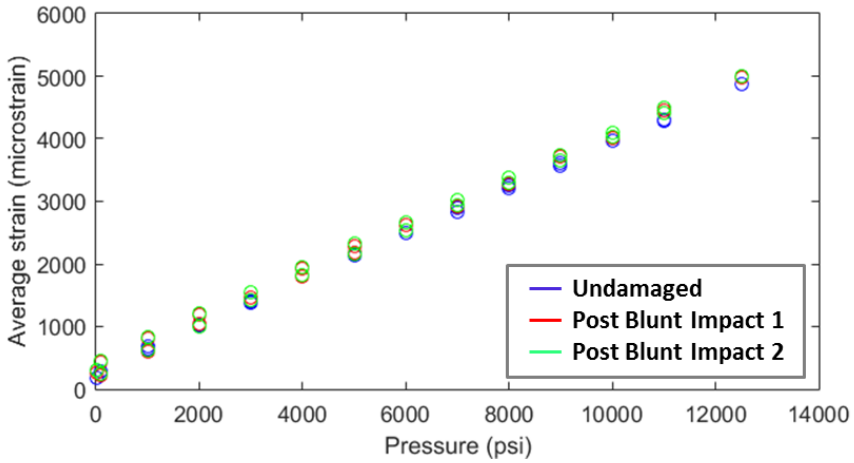

Figure 9. Average strain over center 2 m of sensor over the full pressure range.
1000 psi = 6.9 MPa.

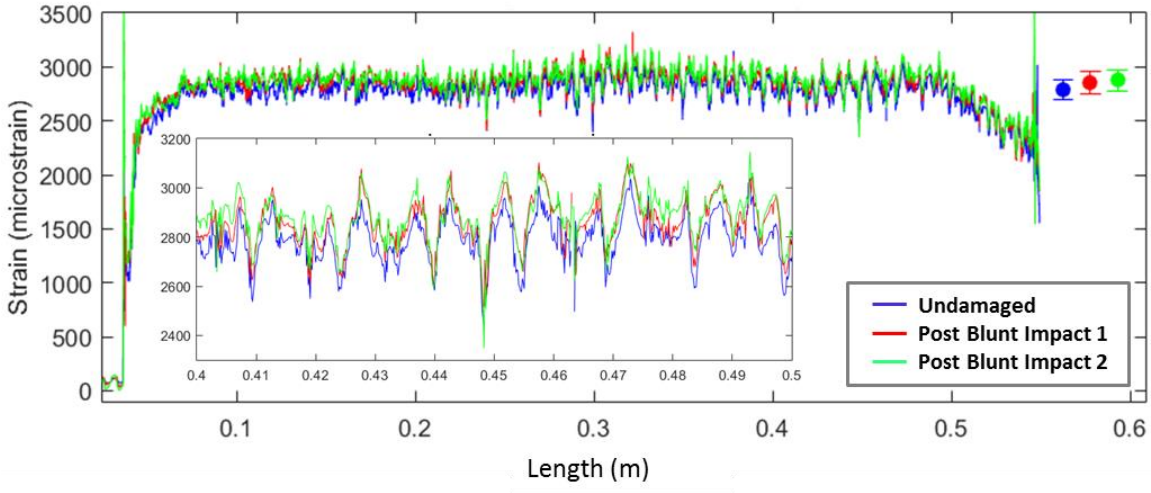

Figure 10. Distributed strain along circumferentially embedded sensor at 7,000 psi (48.3 MPa) before damage and after Impacts 1 and 2. Average strain along the center 2 m is plotted as a point for each data set with 95 % uncertainty bars around each.

3.3 Highly Localized Damage

Following blunt impact damage, the COPV was exposed to a point stress concentrator (a 0.25 cm deep x 1 cm long slot milled into the composite overwrap at about the 0.35 m location) and additional localized impact damage at the same location, shown in Figure 11.

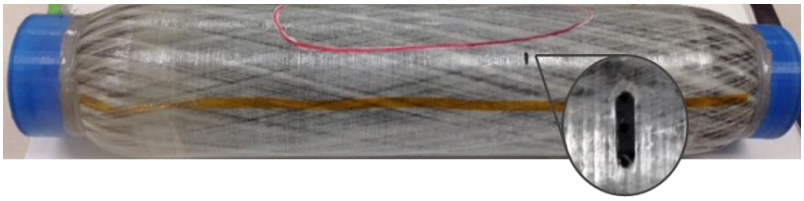

Figure 11. Point stress concentrator and location of localized impact damage.

Results from pressure testing are shown in Figure 12, over a region encompassing the damage. After the pressure vessel was subjected to the stress concentrator and sharp impact, residual stress could be seen in the strain profile in the unpressurized vessel. Unlike the blunt impact damage results, here sharp strain concentrations spread away from the actual defect area, and persist as the vessel is pressurized to 2,000 psi. Strain contours plotted in Figure 12 (c) show a much more concentrated region of compression than in the blunt impact contour plot, with lower amplitude tension broadly surrounding the compressed region. It is possible that the impact locally buckled the aluminum liner, already in compression as a result of the autofrettage. Hydrostatic testing of this damaged COPV up to 12,500 psi resulted in a total expansion of 139 cc and a permanent expansion of 3 cc. This permanent expansion is only 2% of the total expansion. Based on the measured data, the testing would not typically result in a rejection of the vessel. This indicates that hydrostatic testing is not sufficiently sensitive to detect this level of highly localized damage, even as fiber sensing and visual inspection are.

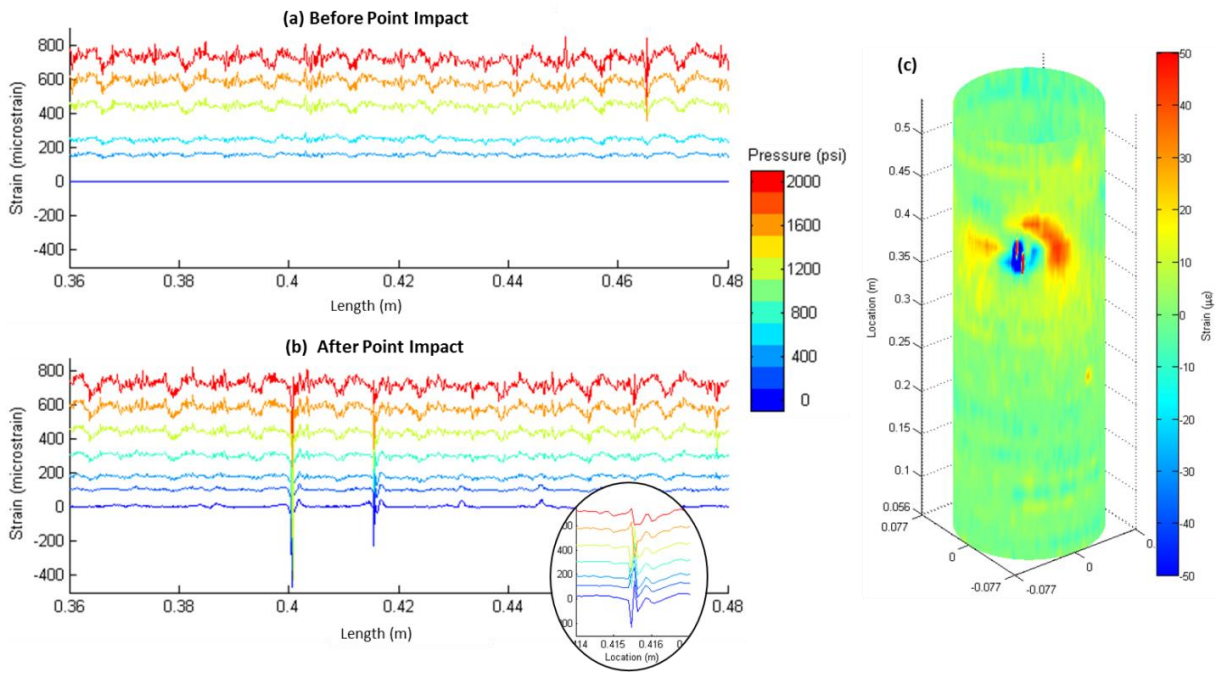

Figure 12. Distributed strain along circumferentially embedded sensor over a range of pressures before (a) and after (b) introduction of localized point damage. The inset provides a zoomed-in view of the damage profile at location 0.4155 m. (c) Strain contours along circumferentially embedded sensor following localized point damage, unpressurized vessel. 1000 psi = 6.9 MPa.

3.4 Distributed Strain-Calculated Volumetric Expansion

Current DOT COPV standards require hydrostatic testing to determine whether changes in volumetric expansion are present which could indicate damage to and potential loss of integrity of the pressure vessel. Distributed strain measurements can similarly be used to calculate volumetric expansion and therefore overall stiffness of the flask; additionally, distributed sensors embedded in different layers of the composite overwrap are capable of detecting changes in load distribution over the lifetime of the vessel as well as the stress ratio in development testing, thereby feeding accurate values of the stress ratio into stress fracture reliability models. Here we show that the portion of volumetric expansion resulting from hoop strain can be calculated from the distributed strain measurements. The vessel is broken down into slices corresponding to the fiber sensor gage length L_0, as shown in Figure 13.

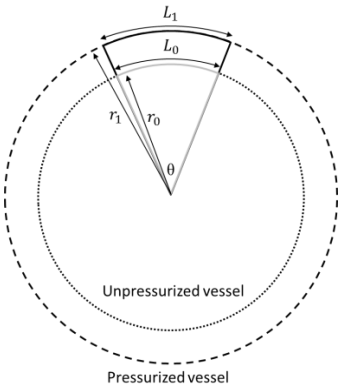

Figure 13. Nomenclature for volumetric expansion calculated from hoop strain over the cylindrical region of the COPV.

Unpressurized, the volume of each slice V_0, with a thickness H, can be expressed as

$$V_0 = \pi r_0^2 * \frac{\theta}{2\pi} * H$$

Thus

$$V_0 = \frac{r_0^2 H\theta}{2}, \quad [1]$$

where r_0 is the initial vessel radius and θ is the angle about the center line of the vessel, created by the arc length L_0.

Upon expansion, the arc length of the slice increases to L_1 as the vessel undergoes expansion. Strain, ε, is then defined as:

$$\varepsilon = \frac{L_1 - L_0}{L_0} \quad [2]$$

Substituting into and rearranging equation [2],

$$\varepsilon = \frac{\theta(r_1 - r_0)}{\theta r_0} \quad [3]$$

$$r_1 = r_0 * (\varepsilon + 1). \quad [4]$$

Calculating the fractional volume change upon pressurizing,

$$\frac{V_1 - V_0}{V_0} = \frac{(r_1^2 - r_0^2)}{r_0^2} \quad [5]$$

$$\frac{V_1 - V_0}{V_0} = \frac{r_0^2(\varepsilon + 1)^2 - r_0^2}{r_0^2}$$

$$\Delta V = \varepsilon(\varepsilon + 2) * V_0 \quad [6]$$

Using the average strain values for the undamaged COPV, a volumetric expansion of approximately 101 cc is calculated, compared with 137 cc from the hydrostatic test. These results are reasonable as we are only calculating the expansion resulting from the component of strain 6° off-axis of the hoop direction for the cylindrical region of the vessel. Contributions from the longitudinal strain as well as the ends of the vessel will further increase the total expansion calculated. For pressure vessels designed to fail in the central cylindrical region, measuring the hoop strain in this area may be sufficient to detect manufacturing defects or in-service damage. If desired, sensors could similarly be embedded in the longitudinal direction and over the end regions of the flask.

3.5 Load-Sharing

Lastly we present data from the sensor located at the carbon-glass interface compared with that from a second strain sensor located within the carbon composite, closer to the metallic liner of the vessel (Figure 14). The difference in slopes of the data clearly shows that the inner-most sensor experiences higher strain as the pressure increases.

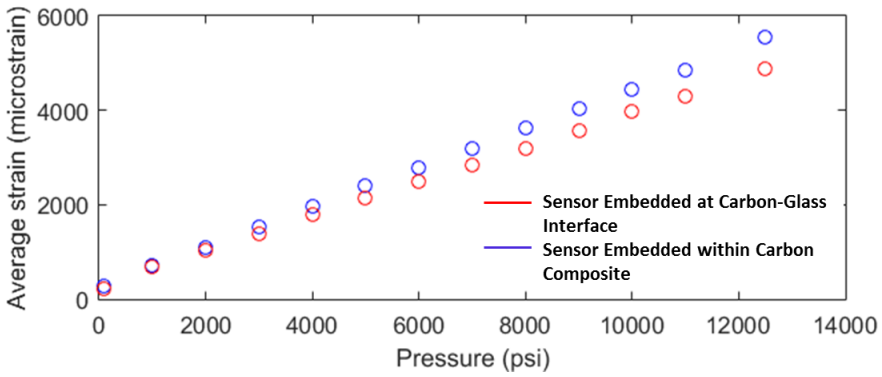

Figure 14. Average strain over 2 m of the embedded sensors at two different depths within the COPV. 1000 psi = 6.9 MPa

4. CONCLUSIONS

Luna, teamed with Worthington Industires, has demonstrated that embedded distributed strain sensors are capable of providing detailed strain profiles over the entire operating pressure range of a COPV, enabling a built-in assessment of the structural integrity of the vessel. High-definition distributed strain sensing was successfully used to monitor strain along the axis of circumferentially embedded fiber optic sensors during qualification testing and following blunt and highly localized damage events to the COPV. The strain profiles revealed and quantified the damage to the vessel.

This easily-embedded sensing technology has the potential to provide designers with a tool for stress reliability model verification, and to provide rapid in-situ assessment of the structural integrity of composite pressure vessels. Damage is easily detectable at thresholds below those resolved by the hydrostatic test; in addition to the potential for replacing hydrotesting, the risk

associated with the use of 30 year extended service life flasks will be mitigated by utilizing this efficient health monitoring capability to identify damage and weakened flask structure.

5. ACKNOWLEDGEMENTS

Luna is sincerely thankful to Worthington Industries (specifically to Robert Sanchez), for their support on this work.

6. REFERENCES

1. McLaughlan, P., Forth,S., and Grimes-Ledesma, L. "Composite overwrapped pressure vessels: a primer." *National Aeronautics and Space Administration, Johnson Space Center*. 2011.
2. Forth, S. "Composite Overwrapped Pressure Vessel Risks." *Technical Memo ES4-08-043*. September 30, 2008.
3. Russel, R., Grundy, D., Jablonski, D., Martin, C., Washabaugh, A., and Goldfine, N. "Health Monitoring of Composite Overwrapped Pressure Vessels (COPVs) using Meandering Winding Magnetometer (MWM®) Eddy Current Sensors". *Proceedings of the 12th International Symposium on Nondestructive Characterization of Materials (NDCM-XII)*. June, 2011.
4. Soller, B., Gifford, D., Wolfe, M., and Froggatt, M. "High resolution optical frequency domain reflectometry for characterization of components and assemblies." *Optics Express* 13 (2005): 666-674.
5. Soller, B. J., Wolfe, M., and Froggatt, M. E. "Polarization resolved measurement of Rayleigh backscatter in fiber-optic components." *Optical Fiber Communication Conference and Exposition and the National Fiber Optic Engineers Conference Technical Digest*. Anaheim, California, March 6, 2005. Optical Society of America, 2005. Paper NWD3. CD-ROM.
6. Kreger, S., Gifford, D. K., Froggatt, M. E., Soller, B. J., and Wolfe, M. S. "High resolution distributed strain or temperature measurements in single- and multi-mode fiber using swept-wavelength interferometry." *Optical Fiber Sensors, OSA Technical Digest.* Cancun, Mexico, October 23, 2006. Optical Society of America, 2006. Paper ThE42. CD-ROM.
7. Castellucci, M., Klute, S.M., Lally, E.M., Froggatt, M.E., and Lowry, D. "Three-Axis Distributed Fiber Optic Strain Measurement in 3D Woven Composite Structures." *Smart Structures/NDE*. San Diego, CA, March 10-14, 2013.
8. Gifford, D., Metrey, D., Froggatt, M., Rogers, M., and Sang, A. "Monitoring Strain During Composite Manufacturing Using Embedded Distributed Optical Fiber Sensing." *SAMPE Technical Conference Proceedings: 2011 – State of the Industry: Advanced Materials, Applications, and Processing Technology.* Long Beach, CA, May 23-26, 2011. Society for the Advancement of Material and Process Engineering.
9. Pedrazzani, J. R., Klute, S. M., Gifford, D. K., Sang., A. K., and Froggatt, M. E. "Embedded and surface mounted fiber optics sensors detect manufacturing defects and accumulated damage as a wind turbine blade is cycled to failure." *SAMPE 2012 Technical Conference Proceedings: Emerging Opportunities: Materials and Process Solutions*. Baltimore, MD, May 21-24, 2012. Society for the Advancement of Material and Process Engineering.